Tectonic significance of Main Central Thrust around Annapurna detected by 3D strain analysis

Tectonic significance of Main Central Thrust around Annapurna detected by 3D strain analysis

Daigoro Hayashi

Simulation Tectonics Laboratory,
Faculty of Science, University of the Ryukyus,
Nishihara, Okinawa, 903-0213, Japan

Abstract

The Main Central Thrust (MCT) zone is one of the most important tectonic zones of the Himalayas along which the inverted metamophism has been observed. The MCT zone around Annapura have been surveyed to analyse 3D strain by adopting the least squre method (Hayashi, 1994,2001). The problem which is encountered in treating 3D strain analysis, is the precision of strain. The consistent value (c-value) was derived to estimate how the resultant value of strain is consistent with true value (Hayashi,1995). Setting the c-value properly, invalid samples are excluded from the strain analysis. The paper summerized as its important result that the foliation plane and XY plane are almost parallel together. Although this result has been recognized as a general agreement by many geologists, there has been no direct proof using 3D strain analysis up to now. Shear heating model is considered as the reasonable cause of inverted metamorphism along the MCT from the intermediate intensity of strain. The 3D strain analysis introduced here has benefits that any rock which is composed of grains can be used as marker rock and we can find out such rocks ubiquitously throughout the Himalayas.

Introduction

One of the important topics of numerical simulation is how to check its results. If we consider the underthrusting of Indian lithosphere beneath the Himalaya and Tibet, this will be done using the earthquake focal mechanisms, distribution of earthquake hypocenter, neotectonic morphology, stress measurement and strain measurement (Chamlagain and Hayashi, 2005). Although there are some 3D strain analysis techniques, none of them are used to examine the simulation results so far.

3D strain was once calculated using the oriented samples collected from Annapurna Region though the result seemed not reasonable (Kawamitsu and Hayashi, 1991). I have performed the calculation again using the same samples by the least square method (Hayashi,1994) and have obtained reasonable strain. The strain shows us a remarkable feature that the foliation plane almost coincides with principal strain XY plane. This strongly suggests that 3D strain analysis is the effective way to check tectonic simulations by comparing the measured and the calculated strains on a same geological profile.

The surveyed region is located in the north of Pokahara around the Annapurna Himal, Central Nepal as shown in Fig.1. The previous works of the area have been published by Ohta et al. (1973), Pecher and LeFort (1977), Kano (1982), Arita (1983), Kawamitsu and Hayashi (1991) and Kaneko (1997). The Main Central Thrust has inclined gently northwards trending east to west and has run subparallel along the Himalayan range. The paper describes the outline of geology, lithology, and three dimensional (3D) finite strain analysis around the Annapurna Himal, and discuss the relationship between the MCT zone and the finite strain.

Received: June 30, 2008

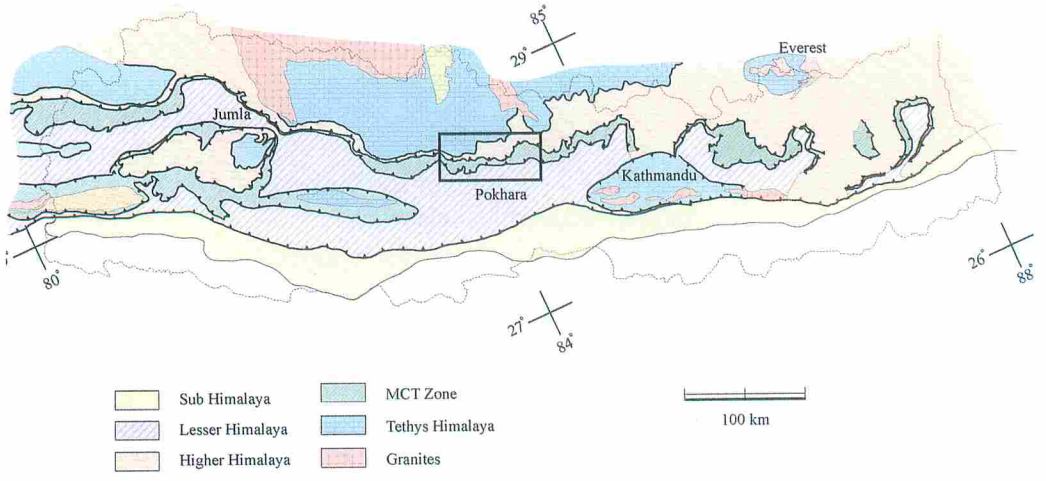

Fig.1 Geological map of Nepal (compiled by Kizaki and Hayashi, 1984)

Geological Setting

Around the Annapurna area, there are four major tectonic units which are called the Lesser Himalaya zone, Main Central Thrust zone (MCT zone), Higher Himalaya zone and Tethys zone from south to north. They strike generally N50° ~80° W dipping 20° ~50° NE (average N75° W, 30° NE) as shown in Fig.2, younger from south to north. Three sections along AA', BB' and CC' are drawn in Fig.3.

The Lesser Himalaya zone consists of low grade metamorphosed rocks such as sandstone, quartzite and phyllite. The zone is bounded on the MCT zone by the lower MCT. The lower MCT has not been recognized

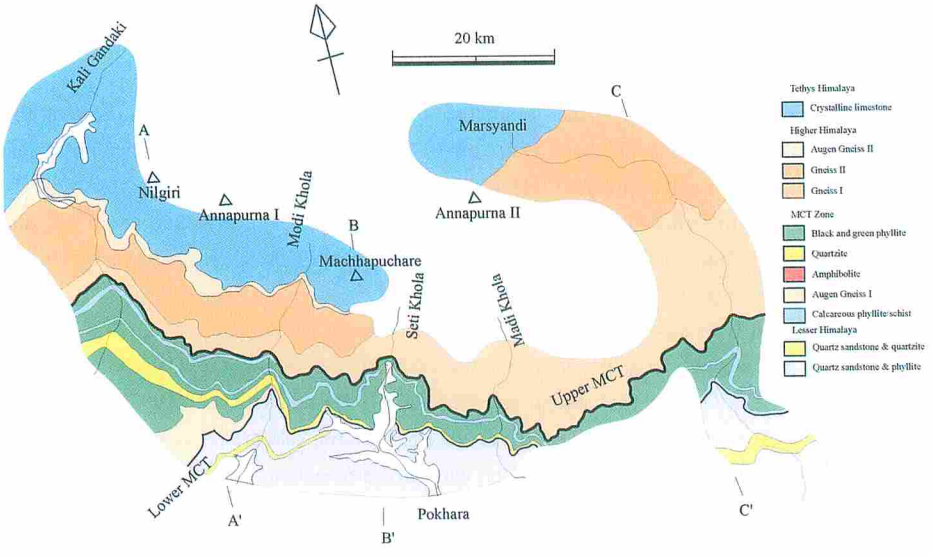

Fig.2 Geological map around Annapurna (modified from Kawamitsu and Hayashi, 1991)

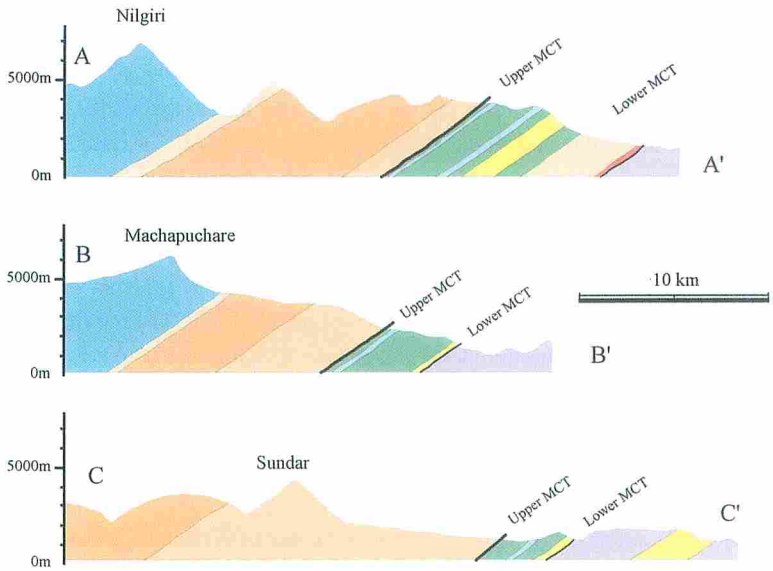

Fig.3 Geological profile around Annapurna (modified from Kawamitsu and Hayashi, 1991)

clearly in the area.

The MCT zone lies between the Higher Himalaya zone and Lesser Himalaya zone. Its northern fringe is bordered by the upper MCT and the southern fringe by the lower MCT, respectively. The upper MCT is clearly recognized by the difference of lithofacies, though the very boundary is obscure. The zone is characterized by low to medium grade metamorphic sheared rocks which are black and green phyllite, quartzite, calcareous rocks and amphibolite.

The Higher Himalaya zone consists of various kinds of gneisses and migmatitic gneiss with augen structure. The zone thrusts over the MCT zone along the upper MCT.

The Tethys zone is composed of low grade metamorphic quartzite, limestone and mudstone, and overlies the Higher Himalaya zone. Their boundaries change gradually and are not recognized directly.

Lithostratigraphy

Lesser Himalaya Group

The group consists of weakly metamorphosed sediments and is overlain by the MCT group. The group is roughly divided into two subgroups; the quartzite and sandstone subgroup, and the sandstone and phyllite subgroup.

The quartzite and sandstone subgroup is mainly composed of quartzite with sandstone interbeds. The quartzite is white in color, including muscovite, biotite and plagioclase. Crenulation cleavages are shown on bedding planes.

The sandstone and phyllite subgroup is mainly exposed in the Lesser Himalaya area. The group consists mainly of biotite bearing black phyllite with quartz veins. Crenulation cleavages and kink folds are seen on the bedding plane.

Main Central Thrust Group (MCT Group)

The group lies between the Higher Himalaya group and the Lesser Himalaya group, being bounded by the

upper Main Central Thrust at the north, the lower Main Central Thrust at the south. The thickness of the group is 2000 m at least. The group has intensely sheared, and consists of the black and green phyllite subgroup, augen gneiss I subgroup, amphibolite subgroup, quartzite subgroup and calcarious phyllite schist subgroup.

The black and green phyllite subgroup is commonly exposed in the area and is composed of biotite-graphite-phyllite, wavy green phyllite and biotite-chlorite phyllitic schist with or without garnet. The phyllitic schist is characterized by wavy micaceous layers with irregularly folded lenticular quartz aggregates. The typical mineral assemblage is garnet-biotite-muscovite-K feldspar-plagioclase-quartz.

The augen gneiss I subgroup is seen at Ulleri along the Kali Gandaki River. The augen gneiss consists of medium- to coarse- grained minerals. The augen structure comprised K feldspar-porphyroblasts and/or porphyroclasts. The gneiss was called Ulleri augen gneiss by Le Fort (1975). The thickness of the subgroup is about 1000 m at least. The representative mineral assemblage is biotite-muscovite-K feldspar-plagioclase-quartz.

The amphibolite subgroup; several amphibolite sheets are placed between the lower and middle parts of the MCT group. The thickness of the sheets is estimated less than 100 m. Typical mineral assemblage is hornblend-biotite-quartz-K feldspar.

The quartzite subgroup; a few quartzite layers are placed between the middle horizons of the MCT group along the Kali Gandaki and Modi Khola Rivers. The thickness of the quartzite varies from several hundred to one thousand meters. The colors of the quartzite are white, bluish grey and green. These quartzites are fine- to medium-grained sand size, including thin micaceous layers (1-5 mm).

The calcareous phyllite-schist subgroup is exposed close to the upper MCT, and thickness of the subgroup is estimated about 150 m.

Higher Himalaya Group

The group consists of various kinds of gneisses and thrusts over the MCT group along the upper MCT. The group is, based on the field survey, divided into three subgroups; gneiss I, gneiss II and augen gneiss II subgroups. Structure of these gneisses is generally concordant with that of the upper MCT. Apparent thickness of the group is about 6000 m at least.

The gneiss I subgroup; basal part of the Higher Himalaya group is composed of the gneiss I subgroup, which is represented by the alternation of pelitic and psammitic gneisses. The pelitic gneiss posseses medium- to coarse-grained minerals, especially garnet which reaches 10 mm in diameter, while the psammitic gneiss consists of fine-grained particles. The typical mineral assemblage is garnet-biotite-muscovite-K feldspar-plagioclase-quartz.

The gneissII subgroup is composed of fine- to medium-grained calc-silicate gneiss and overlies the gneiss I subgroup. The change from the gneiss I to gneiss II subgroup is gradual. Thickness of the subgroup is 2000 m at least. The subgroup is usually layered with whitish to greenish quartzose feldsparthic gneissosity which varies from 5 mm to 20 mm in thickness. Ptygmatic folds are sometimes seen. The typical mineral assemblage is biotite-muscovite-kyanite-calcite-plagioclase-quartz.

The augen gneiss II subgroup, which is composed of migmatitic gneiss with augen structure, occupies the upper part of the Higher Himalaya group. The subgroup is developed along the Kali Gandaki and Modi Khola Rivers. The thickness is 400 m at least. The subgroup is characterized by the augen structure whichi is made of lenticular and euhedral quartz and K feldspar porphyroblasts or aggregates with maximum length 2 cm in longitudinal side. The augen is elongated in parallel or subparallel to the foliation. The typical mineral assemblage is biotite-muscovite-K feldspar-quartz.

Tethys Group

The group is composed of the crystalline limestone subgroup and the alternation of quartzite and mudstone subgroup. The group overlies the Higher Himalaya group and seems to be intensely deformed. The wavelength of folding of several kilometers can be recognized. The group is called the Larjung Formation by Bordet et al. (1981). Thickness of the group is more than 2000 m.

The crystalline limestone subgroup; basal part of the Tethys group is represented by the nonfossiliferous crystalline limestone subgroup. Thickness of the subgroup is 1000 m at least.

The alternation of quartzite and mudstone subgroup overlies the crystalline limestone subgroup. The interval of alternation varies from several cm to several m. Thickness of the subgroup is 1000 m at least.

Method of Strain Analysis

Sampling

Fifty pieces of oriented samples are collected around the southern area of the Annapurna Range, and twenty five samples are finally chosen (Fig.6). Because thirteen pieces of them are calcareous schists and

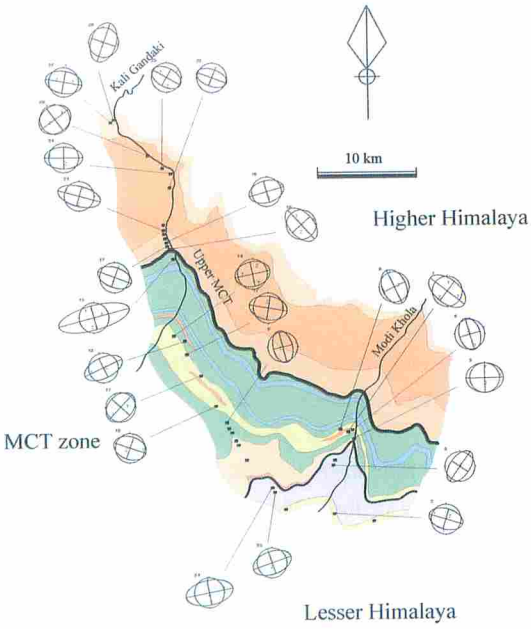

Fig.6 Strain ellipsoid along Kali Gandaki and Modi Khola

gneisses of which grain size is too large to use for strain analysis, the rest thirty six samples are analysed for 3D strain. As eleven of them have high c-value (refer to discussion), they are excluded from the analysis.

Treatment of samples in laboratory

Samples were cut into cubes with edges of approximately 5～10 cm. Each side is named as A, B and C planes, where these planes share common one apex and form nearly right angles together (Fig.5). Thin sections are made from the rectangular pieces and their photographs are taken through microscope (×40). Fifty to two hundred ellipses are drawn adjusting to the shape of quartz grains for each thin section.

Strain ellipses on oriented sample

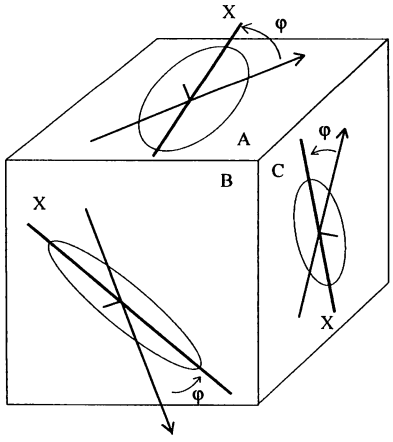

Fig.5 Strain ellipses marked on oriented sample

Strain analysis

Strain analysis is divided to two parts, one is 2D and the other is 3D strain calculation. Shape of quartz grain is used as strain marker which is assumed to deform from its initial ellipse to the final ellipse.

2D strain analysis

The fabric method (Wheeler, 1986) is used for 2D strain analysis where calculation is performed by computer, since the method does not need the graphical and other manual operations but needs algebraic treatment only. On the contrary, if the Rf/ϕ method (Ramsay, 1967; Dunnet, 1969; Dunnet and Siddans, 1971; Lisle, 1977, 1985) is taken, it is formidable by inevitable manual interruption.

Figure 4 explains the fabric method. Marker ellipses are deformed by "deformation tensor D" . The deformed marker ellipses are averaged into a fabric ellipse. On the other hand, we can caluculate a strain ellipse from the deformation tensor D. The fabric method maintains that the fabric ellipse is identical to the strain ellipse under the next four conditons. (1) Initial shape of marker is ellipse.(2) There is no initial foliation within markers.(3) There is no competency contrast between markers and matrix.(4) Markers are deformed in homogeneous finite strain. (Wheeler, 1986).

3D strain analysis

Least square method (Hayashi, 1994,2001) is used for 3D strain analysis. After the 2D strain analysis, we have already obtained the direction of long axis and the axial ratio of the strain ellipses on the planes A, B and C as shown in Fig.5. The following procedure is necessary to obtain the 3D strain.

(1) Calculate the relative axial length of the strain ellipses by GS method (refer Hayashi, 1994,2001).

(2) Calculate the shape tensor of the strain ellipsoid that is constructed from the strain ellipses by the least square strain technique.

(3) Calculate the axial lengths X, Y and Z using the eigen values of the shape tensor of the strain ellipsoid.

Fabric method

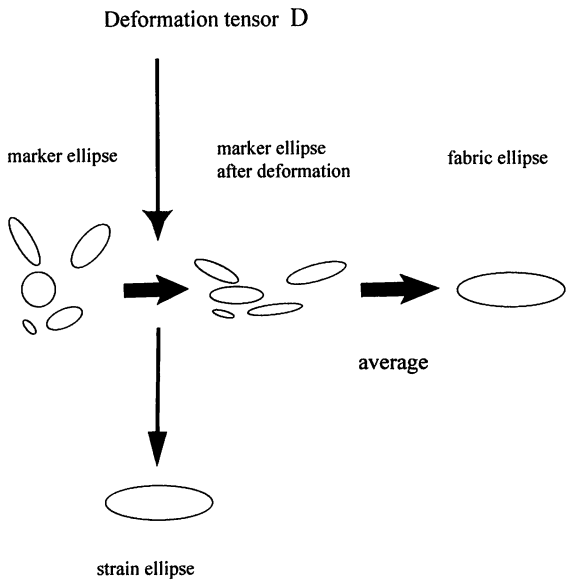

Fig.4 Fabric method

Supposing that λ_1 , λ_2 and λ_3 are the eigen values of the shape tensor and that $\lambda_1 \leq \lambda_2 \leq \lambda_3$

,we have the axial lengths of the strain ellipsoid as

$$X = \sqrt{\frac{1}{\lambda_1}}, \qquad Y = \sqrt{\frac{1}{\lambda_2}}, \qquad Z = \sqrt{\frac{1}{\lambda_3}}$$

,where X>Y>Z.

(6) Calculate the direction of X, Y and Z of the strain ellipsoid using the eigen vectors of the shape tensor. The direction of X, Y and Z equals that of the eigen vectors which correspond with λ_1 , λ_2 and λ_3, respectively.

Results of Strain Analysis

Figure 6 shows three principal strain axes X, Y and Z on the lower hemisphere of equal area projection (25 points) around Kali Gandaki and Modi Khola. The great circle shows the circle of Schmidt net and X, Y and Z are three principal strain axes. Center of the symbols of X, Y and Z indicates its direction on the Schmidt net. Accompanied ellipse indicates XZ plane of strain ellipsoid which is really on an inclined plane but is drawn as if on an horizontal plane from which we recognize the ratio of length of X and Z.

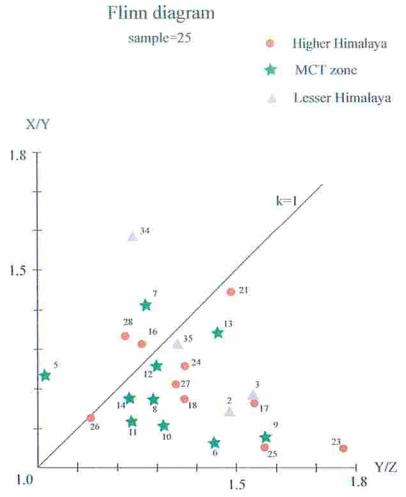

Fig.7 Flinn diagram. A point of sample number 15 is out of this range.

Flinn diagram

Figure 7 is the Flinn diagram which shows: (1) Intensity of strain of Higher Himalayan and Lesser Himalayan rocks is larger than that of MCT zone rock. (2) Six samples belong to the prolate type and the other nineteen samples to the oblate type, so that there are meaningful difference in the distribution of strain type. (3) One prolate type strain ellipsoid (sample number 15) shows extraordinarily high value which is out of Fig.7.

Orientation of strain axis and foliation

Figures 8a and b show the orientations of Z axis of strain and pole of foliation in the three zones, respectively. Figures 9a, b and c compare both orientations of Z axis and foliation pole for samples of Higher Himalaya, MCT zone and Lesser Himalaya, respectively. The tied lines show the difference between both orientations of

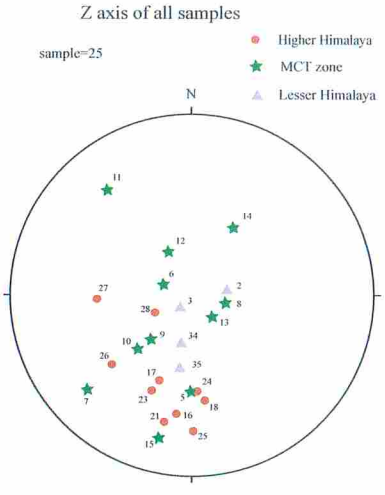

Fig.8a Z axis of strain

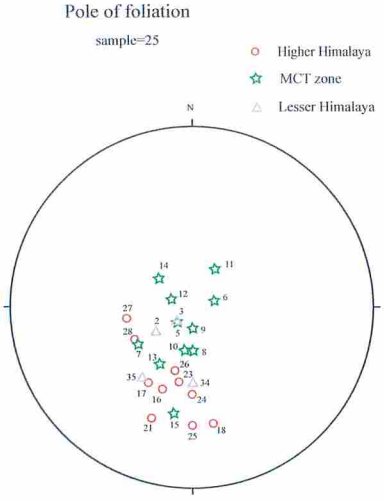

Fig.8b Pole of foliation

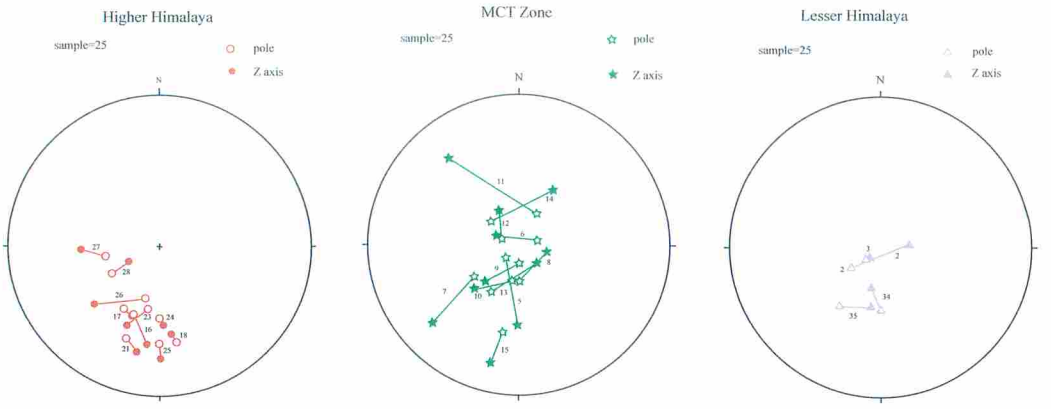

Fig.9 Angle deviation between pole of foliation and Z axis of strain
a: Higher Himalaya, b: MCT zone, c: Lesser Himalaya

Z axis and foliation pole. The length of the tied lines shows that it is short in the Higher Himalayan samples and is longer in the MCT zone and Lesser Himalaya. Thus, the orientation difference in the Higher Himalaya is smallest. The orientation difference is small in the MCT zone, while it is larger than that in the Higher Himalaya. The orientation difference in the Lesser Himalaya is small, though the sample number is only four. Three figures 9a, b and c show that XY plane is almost parallel to the foliation plane, as we know, since the Z axis is the pole of XY plane.

2D strain on profile along NE to SW

In order to consider the relation of strain ellipse and foliation plane on a profile plane, distribution of strain ellipses is drawn by projecting strain ellipsoids onto the NE-SW section A-A' as shown in Figs.10a,b,c,d. Strain ellipsoids of twenty two samples are projected on the section A-A', where it seems that the XY planes of fifteen samples are parallel to the foliation, planes of which dip ca. 35° NW, and for the other seven samples the XY planes seem oblique to the general inclination of foliation planes.

Discussion

consistent value (c-value)

We should consider one problem when we construct an ellipsoid from three ellipses. Figure 11 shows an ellipsoid where we set up coordinate axes x, y and z as intersections among three ellipses. Figure 12 shows three ellipses in plan view. Since the length of axis from the center of ellipse to the surface line of ellipse is same in all the ellipses, the same colored arrows must have proportionally the same length. If three ellipses are the parts of one ellipsoid, the relation $r = \frac{p}{q}$ hold, though actually the relation does not hold. In order to show how much the discrepancy is, we introduce the consistent value (c-value).

$$c = \frac{l_{pq} - l_r}{l_{pq}} = 1 - \frac{qr}{p}$$

If c-value is zero, three ellipses are exactly the parts of one ellipsoid and the ellipsoid is considered true strain ellipsoid. As c-value deviates from zero, the ellipsoid diverges from true strain ellipsoid. The next

problem is how we introduce as the threshold c-value over which the ellipsoid is invalid as a strain ellipsoid. In the paper I have taken the threshold value being 0.3. Then the number of valid samples decreases from thirty six to twenty five. Thus, we can exclude the invalid samples from 3D strain analysis.

Relation between fabric and strain

The relations between the fabric pattern and the orientation of the principal axes of strain ellipsoid are interesting subjects. One of the subjects is a problem whether the strain field is consistent with the foliation plane or not. The relation of 3D direction between the pole of foliation and the Z axis of strain is shown in Fig.9a,b and c. As I have already described, the foliation plane and the XY plane are nearly parallel.

2D strain feature on the section A-A' has also answered this question. The XY plane of eleven samples is parallel to the foliation plane, though the X axis of seven samples doesn't seem like parallel to the foliation but obliques nearly 90° from the foliation line as shown in Fig.10. On the contrary, if we examine the X axis of strain ellipses in the outcrop scale, the foliation is really folded to be nearly parallel to the X axis. The difference between foliation and X axis is small and the foliation and XY plane are almost parallel. This means that the obtained strain field has reflected the formation of foliation.

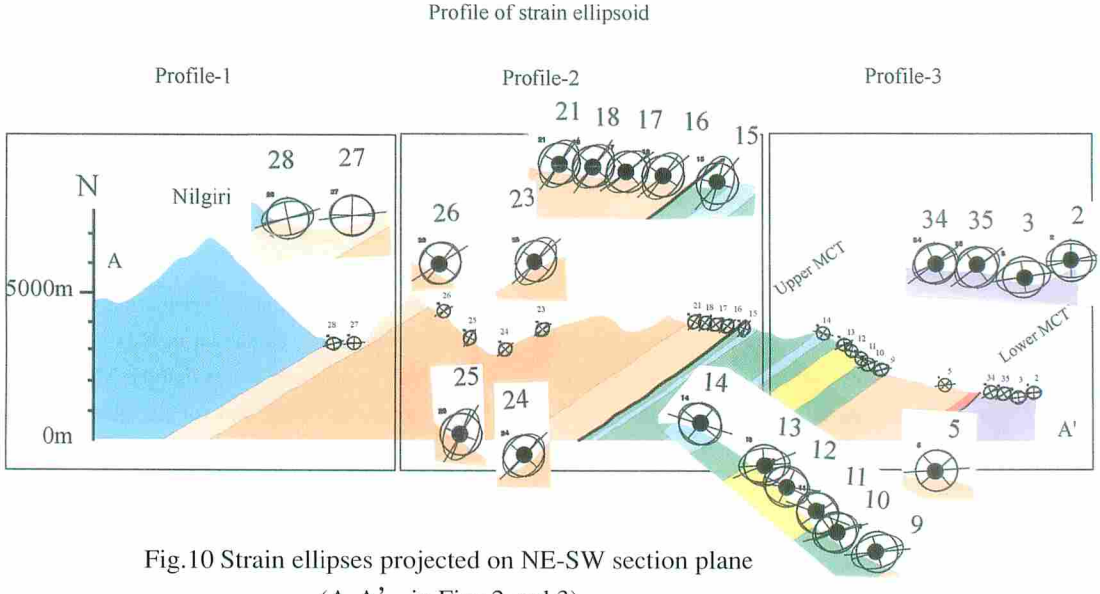

Fig.10 Strain ellipses projected on NE-SW section plane (A-A' in Figs.2 and 3)

Relation to the inverted metamophism

The Main Central Thrust demarcates the Lesser Himalaya zone and the Higher Himalaya zone in the Himalayan Metamorphic Belt. The MCT has been the cause of the inverted metamorphism where the metamorphic grade has increased toward the MCT in the footwall and the Higher Himalaya zone rocks have suffered retrograde metamorphism in the hangingwall (Arita, 1983; Jain et al., 2002). Many explanations have been proposed to solve the inverted metamorphism. (1) Hot-over-cold model (Le Frot, 1975). (2) Shear heating model (Scholtz, 1980; Le Fort, 1986; Arita, 1983). (3) Leucogranite emplacement model (Le Fort, 1986; Pecher, 1989; Searle and Rex, 1989). (4) Post-metamorphic overturned and recumbent fold model (Searle and Rex, 1989) (5) Ductile shearing (Jain and Manickavasagam, 1993).

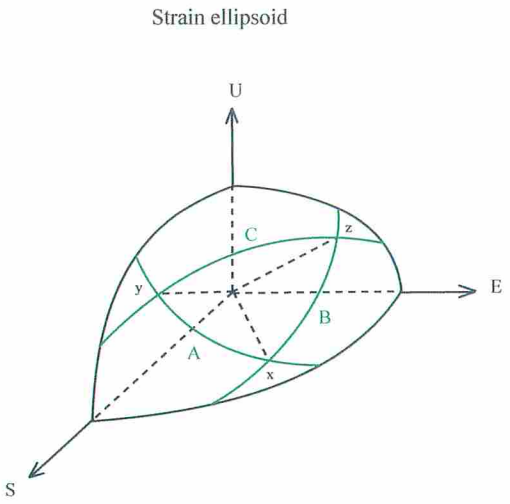

Fig.11 A strain ellipsoid composed with three ellipses A, B and C

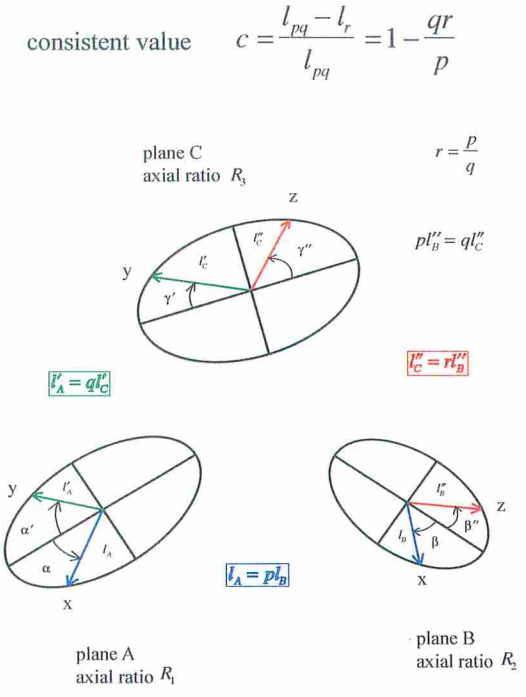

Fig.12 Geometrical relation among three ellipses A, B and C

Figures 13 and 14 show that the $\bar{\varepsilon}_s$ value has indicated intermediate value near along the MCT and the prolate type strain has emerged from near along the MCT, respectively. The value $\bar{\varepsilon}_s$ is called "Nadai's amount of strain" and is defined as

$$\bar{\varepsilon}_s=\frac{\sqrt{3}}{2}\bar{\gamma}_{oct} \quad \text{where} \quad \bar{\gamma}_{oct}=\frac{2}{3}\sqrt{(\varepsilon_1-\varepsilon_2)^2+(\varepsilon_2-\varepsilon_3)^2+(\varepsilon_3-\varepsilon_1)^2} \quad \text{and}$$

$$\varepsilon_1=\ln(1+e_1),\ \varepsilon_2=\ln(1+e_2),\ \varepsilon_3=\ln(1+e_3)$$

which indicates the relative intensity of strain. Considering the result of 3D strain analysis, I have inclined to agree the shear heating model as a cause of the inverted metamorphism. One reason is based on the fact that if shear heating occurred along the MCT, the strain are released to change its intensity low. This is consistent with the intermediate strain intensity near the MCT as shown in Fig.13. The other is that the prolate strain has emerged along the MCT for its long axis being paralell to the stretching of the MCT as illustrated in Fig.14. The prolate strain are apparently caused by simple shear that the hangingwall have driven top-to-southwest sense of movement.

Benefit for Himalayas

The benefits of this 3D strain analysis method are; (1) many kinds of rock which consist of grains, i.e. sandstone and metamorphic rocks derived from sandstone can be treated as marker rock and (2) almost everywhere we can find such rocks in Himalayas.

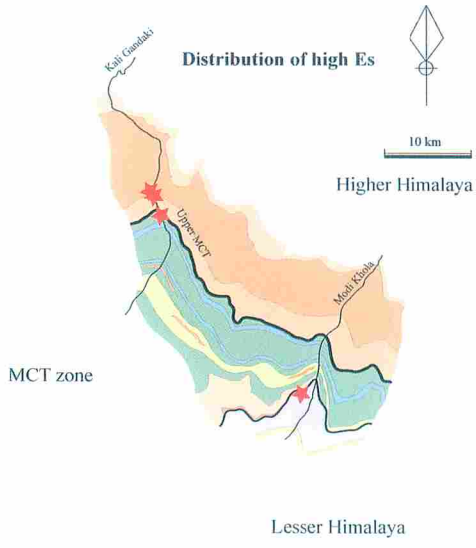

Fig.13 Distribution of intermediate strength $\bar{\varepsilon}_s$ along Kali Gandaki and Modi Khola

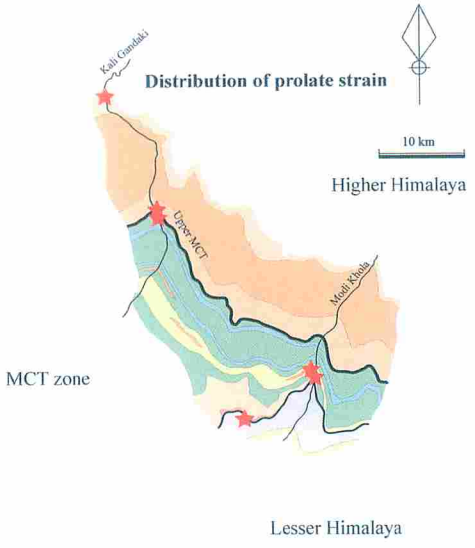

Fig.14 Distribution of prolate type strain along Kali Gandaki and Modi Khola

Refereces

Arita,K., 1983. Origin of the inverted metamorphism of the Lower Himalayas, central Nepal. Tectonophysics, 95, 43-60.

Bordet, P., Colchen,M., Le Fort, P. and Pecher, A., 1981. The geodynamic evolution of the Himalaya. Ten years of research in Central Nepal Himalaya and some other regions. In: Gupta, H.K. and Delany, F.M. eds. Zagros.Hindu Kush.Himalaya Geodynamic evolution, Am.Geophys.Union, 149-168.

Chamlagain,D. and Hayashi,D., 2005. Fault development in the Thakkhola half graben: insights from numerical simulation. Bulletin of the Faculty of Science, University of the Ryukyus, 79, 57-90. (http://ir.lib.u-ryukyu.ac.jp/)

Dunnet,D., 1969. A technique of finite strain analysis using elliptical particles. Tectonophysics, 7, 117-136.

Dunnet,D. and Siddans,A.W.B., 1971. Non-random sedimentary fabrics and their modification by strain. Tectonophysics, 12,307-325.

Hayashi,D., 1994. Three dimensional finite strain analysis techniques from strain ellipses on non-parallel sections. Jour.Geol.Soc.Japan, 100, 150-161. (in Japanese with English abstract) (http://ir.lib.u-ryukyu.ac.jp/)

Hayashi,D., 1995. Proposed consistency c-value for strain ellipsoids in geological structure analysis. Geoinformatics, 6, 13-29. (in Japanese with English abstract) (http://ir.lib.u-ryukyu.ac.jp/)

Hayashi,D., 2001. The technique that constructs strain ellipsoid from three strain ellipses measured on non-parallel sections based on the least square method and the factors that control precision of strain. Bulletin of the Faculty of Science, University of the Ryukyus, 71, 47-70. (http://ir.lib.u-ryukyu.ac.jp/)

Jain,A.K. and Manickavavasagam,R.M., 1993. Inverted metamorphism in the intracontinental ductile shear zone during Himalayan collision tectonics. Geology,21,407-410.

Jain,A.K., Sandeep Singh and Manickavavasagam,R.M., 2002. Himalayan collision tectonics. Gondwana Research Group, Memoir no.7, 114p.

Kaneko,Y., 1997. Two-step exhumation model of the Himalayan metamorphic Belt, central Nepal. Jour.Geol.Soc.Japan, 103, 203-226.

Kano,T., 1982. Geology and structure of the main central thrust zone of the Annapurna range, Central Nepal Himalayas. Jour.Nepal Geol.Soc. vol.2, Special Issue, 31-50.

Kawamitsu,K. and Hayashi,D., 1991. Geology and three dimensional finite strain analysis around Annapurna Himal,Cental Nepal. Bulletin of the Faculty of Science, University of the Ryukyus, 52, 37-52. (http://ir.lib.u-ryukyu.ac.jp/)

Le Fort, P., 1975. Himalayas : the collided range. Am.Jour.Sci., 275(A), 1-44.

Le Fort,P., 1986. Metamorphism and magmatism during the Himalayan collision In:Cowards,M.P. and Ries,A.C.(Eds.) Collision Tectonics.Gelo.Soc.London. Spec.Publ. No.19,159-172.

Lisle,R.J., 1977. Clastic grain shape and orientation in relation to cleavage from the Aberystwyth grits, Wales. Tectonophysics, 39, 381-395.

Lisle,R.J., 1985. Geological strain analysis ; A manual for the Rf/ϕ method. 99p.Pergamon.

Ohta,Y. Akiba,C., Arita,K. and Maruo,Y.,1973. Pokhara-Gurkha region. In: Hashimoto, S. et al., eds., Geology of the Nepal Himalayas. Saikon, Tokyo, 159-188.

Pecher, A., 1977. Geology of the Nepal Himalaya: Deformation and petrography in the Main Central Thrust Zone. Colloque Internat. No.268 Himalaya, Paris 1976, CNRS, vol. Sci. de la Terre, 301-318.

Pecher,A. and Le Fort, P., 1977. Origin and significance of the Lesser Himalaya augen gneises. Colloque Internat. No.268 Himalaya, Paris 1976, CNRS, vol. Sci. de la Terre, 319-329.

Pecher,A., 1989. The metamorphism in the central Himalaya. J.Metam.Geol.,7,31-41.

Ramsay, J.G., 1967. Folding and fracturing of rocks. 568pp, McGraw-Hill.

Scholtz,C.H., 1980. Shear heating and the state of stress on faults. Jour.Geophy.Res.,85,6174-6184.

Searle,M.P. and Rex,A.J.,1989. Thermal model of the Zanskar Himalaya. J.Metam.Geol.,7,124-134.

Wheeler,J., 1986. Average properties of ellipsoidal fabrics: implications for two- and three- dimensional methods of strain analysis. Tectonophysics, 126, 259-270.